

Cite this: *Soft Matter*, 2012, **8**, 9406

www.rsc.org/softmatter

PAPER

Theory of DNA–cationic micelle complexation

Helmut Schiessel,^{*a} María D. Correa-Rodríguez,^b Sergii Rudiuk,^{cd} Damien Baigl^{de} and Kenichi Yoshikawa^c

Received 15th March 2012, Accepted 3rd July 2012

DOI: 10.1039/c2sm25603g

We present a theory of spherical micelle formation from cationic amphiphiles in the absence and in the presence of DNA. The distribution of micelle sizes as well as the critical micelle and aggregation concentrations (cmc and cac) are calculated. Micelle formation is favored by the hydrophobic tails but disfavored by the entropic cost associated with counterion condensation. Counterion release drives the complexation between DNA and amphiphiles and causes micellation at a much smaller concentration than in the absence of DNA. The stiffness of double-stranded DNA favors the formation of large micelles leading to a bimodal distribution of micelle sizes.

1 Introduction

Eucaryotic DNA molecules are centimeters long but need to fit into micron-sized nuclei. This is achieved by the complexation of DNA with cationic histone proteins into nucleosomes resulting in a dramatic compaction of DNA.¹ In a nucleosome, one and three quarter DNA are wrapped along a left-handed helical wrapping path leading to a complex with 10 nm diameter. To learn more about the generic properties of such systems it is interesting to go beyond the nucleosome with its given fixed geometry. This has been achieved by studying the complexation between DNA and cationic spherical nanoparticles of varying sizes.^{2,3}

Another widely studied problem is the complexation between cationic surfactants and DNA.^{4–18} The resulting complexes are of interest as non-viral vectors to deliver genes into cells. These complexes might, however, also be useful as model systems to study DNA-wrapped complexes with a lipid core that can adjust its size over a wide range of values. This goes beyond the histone-inspired nanoparticles^{2,3} that cannot adjust their diameter in response to DNA wrapping. Previous theoretical studies of complexes between polyelectrolytes and micelles modeled the micelles as rigid spheres with a fixed diameter and thus could not study this effect.^{19–22} A different approach, a self-consistent field lattice model,²³ allowed for micelles of various aggregation numbers but could not include chain rigidity.

DNA–cationic lipid complexes show typically a critical aggregation concentration (cac) far below the critical micelle concentration (cmc).^{11,12,14,16,18} Both cmc and cac decrease with

increasing length of the hydrophobic tail of the surfactant.^{11,12,14,16,18} Addition of salt has opposite effects on cmc and cac: the cac increases but the cmc decreases.^{12,15}

Complexes between double-stranded DNA (dsDNA) and cationic surfactants show various morphologies. For instance, the Safinya group found lamellar⁸ and inverted hexagonal phases.⁹ The transition between these phases was achieved through the addition of a neutral lipid that induces a spontaneous curvature of the lipid monolayer or through the addition of a small membrane-soluble cosurfactant molecule that reduces the membrane bending rigidity. In another study it was found that complex formation between dsDNA and cationic lipids leads to rodlike micelles whereas the much softer single-stranded DNA (ssDNA) binds to spherical micelles.²⁴ There are many other parameters that influence the complex morphologies such as the geometrical shape of the individual surfactant molecules, the size and degree of solvation of the counterions and the length of the DNA molecules. This makes it hard to build a general phase diagram showing various structures. Instead we shall assume to be within a range of parameters that favor the formation of spherical micelles wrapped by dsDNA. To achieve this one needs to be in a parameter range far enough from a second cmc that marks a sphere-to-rod transition.^{25,26} In addition, one might choose DNA that is sufficiently short so that its wrapping length around a spherical micelle is comparable to its total length, *i.e.*, for chain lengths much shorter than that of *e.g.* viral DNA⁵ but longer than that of the very short oligonucleotides used in some experiments.^{27,28}

After discussing the geometry of spherical micelles in Section 2, we discuss in Section 3 the energetics of cationic micelles that is governed by the hydrophobicity of the surfactant tails and by the charges of their heads. In Section 4 we calculate the distribution of micelle sizes and the dependence of the cmc on the tail length and the ionic strength. Finally, in Section 5 we add DNA to our model and study the influence of DNA stiffness and counterion release on the distribution of micelle sizes and the cac.

^aInstituut Lorentz, Universiteit Leiden, P.O. Box 9506, 2300 RA Leiden, The Netherlands. E-mail: schiessel@lorentz.leidenuniv.nl

^bPhysics Department, School of Sciences, National Autonomous University of México (UNAM), México, México

^cDepartment of Physics, Graduate School of Science, Kyoto University, Kyoto, 606-8502, Japan

^dDepartment of Chemistry, Ecole Normale Supérieure, 75005 Paris, France

^eUniversité Pierre et Marie Curie Paris 6, 75005 Paris, France

2 Micelle geometry

We assume in the following that the amphiphiles consist of a single hydrocarbon chain with a terminal hydrophilic cationic group. The association of the hydrocarbon tails of several molecules leads to the formation of a micelle core. We define n_C as the number of carbon atoms in the alkyl chain. Following Tanford²⁹ we assume that the CH₂ group adjacent to the polar head lies within the hydration sphere of the headgroup. The volume of the hydrophobic core is then estimated as follows:

$$v_{\text{tail}}(n_C) = v_{\text{CH}_3} + v_{\text{CH}_2}(n_C - 1) \quad (1)$$

with $v_{\text{CH}_3} = 27.4 \text{ \AA}^3$ and $v_{\text{CH}_2} = 26.9 \text{ \AA}^3$. We assume in the following that the micelle is spherical. The radius of the core of such a micelle with aggregation number m is then given by:

$$r(m, n_C) = \left(\frac{3mv_{\text{tail}}(n_C)}{4\pi} \right)^{1/3} \quad (2)$$

Spherical micelles have a maximal possible radius that follows from the length of the alkyl chain:

$$r_{\text{max}}(n_C) = l_{\text{CH}_3} + l_{\text{CH}_2}(n_C - 1) \quad (3)$$

with $l_{\text{CH}_3} = 1.5 \text{ \AA}$ and $l_{\text{CH}_2} = 1.265 \text{ \AA}$.²⁹ This leads to a maximal aggregation number:

$$m_{\text{max}}(n_C) = \frac{4\pi(r_{\text{max}}(n_C))^3}{3v_{\text{tail}}(n_C)} \quad (4)$$

Another geometrical quantity of interest is the area per amphiphile at the distance of closest approach of water molecules to the micellar core. This is given by

$$A(m, n_C) = \frac{4\pi}{m} (r(m, n_C))^2 \quad (5)$$

3 Energetics of cationic micelles

The free energy ΔF of transfer of an amphiphile molecule from the monomeric state to a micelle of aggregation number m is the sum of three contributions:

$$\Delta F(m, n_C) = \Delta F_{\text{tail}}(n_C) + \Delta F_{\text{surf}}(m, n_C) + \Delta F_{\text{el}}(m, n_C) \quad (6)$$

Here the first term is the free energy gained by transferring the tail from the aqueous medium to the hydrophobic core:

$$\Delta F_{\text{tail}}(n_C) = -u_{\text{CH}_3} - u_{\text{CH}_2}(n_C - 1) \quad (7)$$

with $u_{\text{CH}_3} = 2000 \text{ cal mol}^{-1}$ and $u_{\text{CH}_2} = 700 \text{ cal mol}^{-1}$.²⁹ These numbers account for both the entropy gain due to water release during micellization as well as the entropy loss due to constraints of the tail inside the micellar core. This m -independent term does not account for residual contacts of the alkyl chains with the solvent at the core surface. Each amphiphile has still an area $A(m, n_C)$, eqn (5), in contact with water. The second term in eqn (6) accounts for this effect:

$$\Delta F_{\text{surf}}(m, n_C) = \sigma(A(m, n_C) - A_{\text{head}}) \quad (8)$$

Here $\sigma = 25 \text{ cal mol}^{-1} \text{ per \AA}^2$ is the interfacial tension between water and alkyl chains and $A_{\text{head}} = 21 \text{ \AA}^2$ is the surface area per chain if the hydrocarbon atoms would be closely packed perpendicular to the water-core surface.

What is left to be discussed is ΔF_{el} , the last term in eqn (6). It describes the electrostatic free energy change when bringing a charged headgroup to a cationic micelle. If the micelle is highly charged, then the major cost comes from counterion condensation. As long as the amphiphile is in the monomeric state it is so weakly charged that it has no condensed counterion. Once the amphiphile has been transferred to the micelle, it increases the charge of the micelle by one. This usually means that a counterion needs to condense onto the micelle. In doing so it enters from the bulk with concentration c_{salt} of free ions to the much denser atmosphere of condensed ions of concentration c_{cond} . This leads to

$$\Delta F_{\text{el}}(m, n_C) = k_B T \mathcal{Q}(m, n_C) f_{\text{cond}}(m, n_C) \quad (9)$$

with the thermal energy $k_B T = 600 \text{ cal mol}^{-1}$ at room temperature. The quantities $\mathcal{Q}(m, n_C)$ and $f_{\text{cond}}(m, n_C)$ are both dimensionless; the first term is related to the entropy change felt by a counterion when going from the bulk to the condensed layer, the latter term gives the fraction of headgroup charges that is neutralized by condensed ions. Specifically^{30,31}

$$\mathcal{Q}(m, n_C) = \ln \left(\frac{c_{\text{cond}}}{c_{\text{salt}}} \right) \approx \ln \left(\frac{m}{4\pi r^2(m, n_C) \lambda_{\text{GC}} c_{\text{salt}}} \right) \quad (10)$$

In the second step we approximate the argument inside the logarithm, $c_{\text{cond}}/c_{\text{salt}}$, by assuming that all m headgroup charges are neutralized by a counterion, a good approximation as long as $m \gg r(m, n_C)/l_B$ (see eqn (12) below). The quantity $l_B = e^2/\epsilon k_B T$ is the Bjerrum length with e the elementary charge and ϵ the dielectric constant of the solvent; in water at room temperature one has $l_B = 7 \text{ \AA}$. The m counterions are confined within a volume $4\pi r^2(m, n_C) \lambda_{\text{GC}}$ where λ_{GC} is the height of the cloud of condensed counterions: the Gouy–Chapman length $\lambda_{\text{GC}} = 2r^2(m, n_C)/(ml_B)$. Hence

$$\mathcal{Q}(m, n_C) \approx k_B T \ln \left(\frac{m^2 l_B c_{\text{salt}}^{-1}}{8\pi r^4(m, n_C)} \right) = 2k_B T \ln \left(\frac{ml_B \kappa^{-1}}{r^2(m, n_C)} \right) \quad (11)$$

with $\kappa^{-1} = 1/\sqrt{8\pi l_B c_{\text{salt}}}$ denoting the Debye screening length. Note that this expression is similar and sometimes identical to classical approaches to charged micelles.^{32–35} For instance, eqn (11) is identical to eqn (70) of ref. 34 including numerical factors (up to higher-order corrections that are negligible in the current system) which follows from an approximate solution of the Poisson–Boltzmann equation for spherical symmetry.³³

The fraction of headgroup charges that is neutralized by condensed ions, $f_{\text{cond}}(m, n_C)$, is given by

$$f_{\text{cond}}(m, n_C) = 1 - \frac{\mathcal{Q}(m, n_C) r(m, n_C)}{2ml_B} \quad (12)$$

This quantity needs to be larger than one for the upper theory to work. In the regime where $f_{\text{cond}} < 0$ there is no counterion condensation and we have to replace eqn (9) by the micelle charging energy $e^2 m l / (2\epsilon r(m, n_C))$. In the numerical calculations shown below we use a crossover function to create a smooth transition between these two limits.

4 Distribution of micelle sizes and the cmc

In this section we calculate the size distribution of cationic spherical micelles and give an analytical expression for the critical micelle concentration (cmc). Detailed balance requires

$$[Z_m] = [Z_1]^m e^{-m\Delta F(m, n_C)/k_B T} \quad (13)$$

where $[Z_m]$ denotes the mole fraction of micelles of size m . We show the distribution of micelle sizes for $n_C = 12$ in Fig. 1 and for $n_C = 16$ in Fig. 2 for various concentrations around cmc. The maximum of the distribution shifts continuously from small to large m -values similar to the behavior of uncharged micelles.²⁹

We define the cmc as the concentration of monomeric amphiphiles at which their concentration equals the concentration of the maximally sized micelles, $m = m_{\max}(n_C)$. This leads to the condition

$$[Z_1]e^{-\Delta F(1, n_C)/k_B T} = [Z_1]^{m_{\max}} e^{-\Delta F(m_{\max}, n_C)/k_B T} \quad (14)$$

that can be rewritten as

$$c_{\text{cmc}} \equiv [Z_1] = \exp\left(\frac{m_{\max}\Delta F(m_{\max}, n_C) - \Delta F(1, n_C)}{(m_{\max} - 1)k_B T}\right). \quad (15)$$

It is well known that the cmc is not uniquely defined. Our definition of the cmc turns out to be the most convenient for the theoretical treatment. It deviates from the traditional definition that the critical micelle concentration is the total concentration of amphiphiles at which 5% reside inside micelles ($m > 1$).²⁹ Our definition of the cmc produces a value that is about 10 times greater than the traditional one.

Eqn (15) fulfills the Klevens equation:³⁶

$$\ln c_{\text{cmc}} = A - Bn_C \quad (16)$$

with A and B being constants. Specifically we find

$$B = u_{\text{CH}_2}/k_B T \quad (17)$$

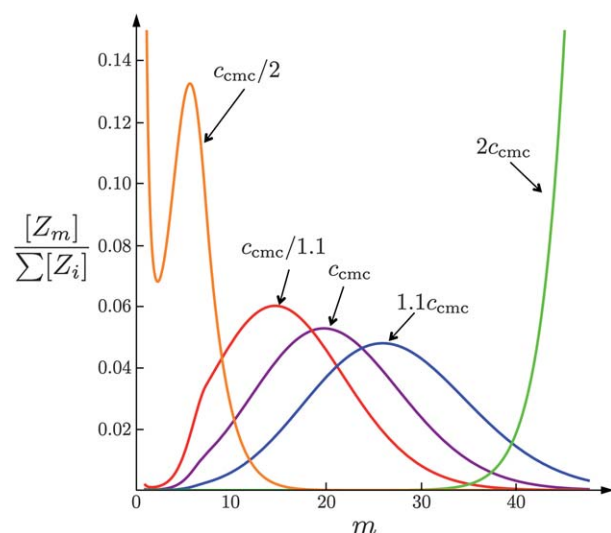


Fig. 1 Size distribution of micelles between $m = 1$ and $m_{\max} = 47$ for tail length $n_C = 12$.

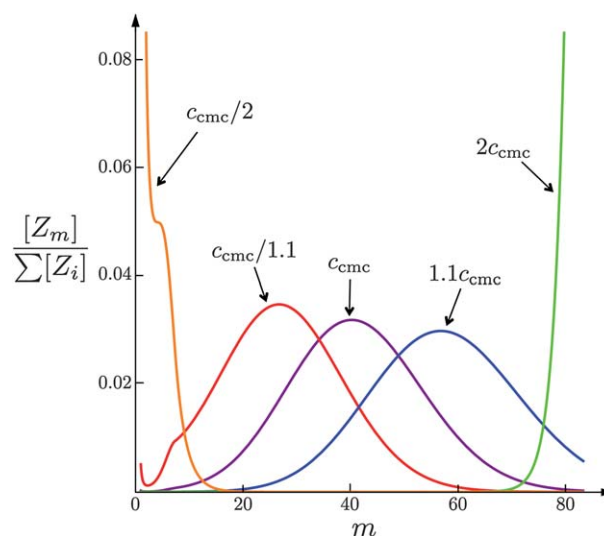


Fig. 2 Size distribution of micelles between $m = 1$ and $m_{\max} = 83$ for tail length $n_C = 16$.

whereas A contains several terms. Strictly speaking, A contains a contribution from the interfacial term, eqn (8), that shows an n_C dependence but this dependence is negligible for two reasons. First of all, the interfacial term is much smaller than the hydrophobic contribution (about $1/10^{\text{th}}$ for reasonable tail lengths). Moreover, it changes very slowly with n_C . For instance, from $n_C = 12$ to infinite tail lengths, $n_C \rightarrow \infty$, the interface term changes only by 2 percent.

Note that A depends on the salt concentration as follows

$$A = \ln\left(\frac{c_{\text{cond}}}{c_{\text{salt}}}\right) + \text{const.} \quad (18)$$

As can be seen from eqn (18) the cmc decreases with increasing ionic strength. This reflects the fact that in order for a micelle to form, it needs to condense counterions. The entropic cost for this process is smaller if the counterion concentration in the bulk is higher. The cmc as a function of the tail length is shown for three different salt concentrations in Fig. 3.

If the salt concentration is very low or if no salt is added, one can replace the cmc with the salt concentration c_{salt} in eqn (10) to

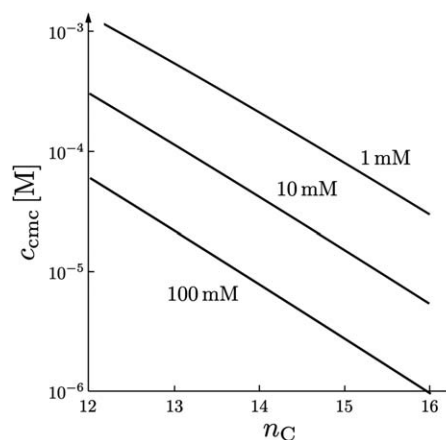


Fig. 3 Tail length dependence of the cmc for three different salt concentrations. Note that the cmc fulfills the Klevens equation, eqn (16).

a very good approximation by c_{cmc} . Bringing $c_{\text{salt}} = c_{\text{cmc}}$ to the other side of eqn (10) one finds

$$B = \frac{1}{2} u_{\text{CH}_2} / k_{\text{B}} T \quad (19)$$

instead of eqn (17) and A is now independent of c_{salt} as long as $c_{\text{salt}} \ll c_{\text{cmc}}$. The slope of $\ln c_{\text{cmc}}$ should therefore change by a factor of 2 when going from low salt to high salt. This has already been pointed out by Konop and Colby³⁷ and has indeed been seen in experiments, see Fig. 1 of the same reference.

5 Influence of DNA on the distribution of micelle sizes and the cac

In this section we consider the role of DNA on the distribution of micelle sizes and the cmc. We expect complex formation between the highly charged DNA molecules and the oppositely charged micelles that is driven by the release of counterions from both DNA and micelles. This should lower the concentration at which micelles form. Moreover, we expect that the size distribution of micelles is affected by the DNA. DNA is a rather stiff molecule with a persistence length of about $l_p = 50$ nm at room temperature. To achieve maximal counterion release, the surfaces of the DNA and the micelle have to be close, so that the counterion atmospheres overlap. Since the corresponding Gouy–Chapman lengths are very small, the DNA has to bend around the micelle if we assume it to stay spherical as we shall do in the following. Since the bending energy of the DNA increases as the inverse of the radius of curvature – here the radius of the micelle – the complex prefers larger micelle sizes. This suggests that – unlike in the DNA-free case – micelles show a bimodal size distribution, monomers or small micelles on one hand and large micelle–DNA complexes on the other hand.

The above-described scenario should be especially effective if the charge densities of the DNA double helix and of maximally sized micelles are comparable. Using eqn (5) we find for micelles with $n_C = 12$ (and above) surface charge densities of about one charge per 63 \AA^2 . This is very similar to the area per phosphate group on the DNA double helix, namely $A_{\text{DNA}} = 107 \text{ \AA}^2$. Micelles with smaller aggregation numbers have smaller charge densities and thus match the DNA charge densities even closer. However, it turns out that micelles that are big enough such that the DNA is able to bend around them, have always surface charge densities that are higher than that of DNA.

The micelle size is typically of similar size as the diameter of the DNA double helix that is given by $2r_{\text{DNA}} = 20 \text{ \AA}$. For instance, $r_{\text{max}}(12) \approx 15 \text{ \AA}$ and $r_{\text{max}}(16) \approx 20 \text{ \AA}$. This excludes multiple wrappings of DNA around the micelle. We assume the wrapping length l_{wrap} (measured here along the line of contact) is on the order of the length of one full turn, namely $l_{\text{wrap}} \approx 2\pi r(m, n_C)$. To achieve such a wrapping length without interference between the two DNA tails the DNA needs to be wrapped along a spiral path (see e.g. Zinchenko *et al.*³).

When the DNA wraps around the micelle, some of the condensed counterions of the micelle and of the DNA are released. We assume that all the fixed DNA charges that come within the micelle's Gouy–Chapman length replace condensed counterions from the micelle and loose their own counterions.

The width of the strip of DNA that is within that distance is given by $w = 2r_{\text{DNA}}\alpha$ where the angle α follows from the law of cosines:

$$\cos \alpha = \frac{(r + r_{\text{DNA}})^2 + r_{\text{DNA}}^2 - (r + \lambda_{\text{GC}})^2}{2r_{\text{DNA}}(r + r_{\text{DNA}})} \quad (20)$$

Using the fact that $\lambda_{\text{GC}} \ll r_{\text{DNA}}$ this can be simplified to

$$\alpha = \sqrt{\frac{2}{1 + r_{\text{DNA}}/r} \frac{\lambda_{\text{GC}}}{r_{\text{DNA}}}} \quad (21)$$

For each released counterion of the DNA one gains (in units of $k_{\text{B}}T$) (Schiessel 01):

$$\Omega_{\text{DNA}} = 2 \ln \left(\frac{2l_{\text{B}}\kappa^{-1}}{r_{\text{DNA}}b} \right) \quad (22)$$

where b is the distance of two charges along the DNA helix, $b = 1.7 \text{ \AA}$.

In total we find the following gain from the counterion release:

$$F_{\text{release}}(m, n_C) = \frac{w l_{\text{wrap}}}{A_{\text{DNA}}} \left[\Omega(m, n_C) + \left(1 - \frac{b}{l_{\text{B}}} \right) \Omega_{\text{DNA}} \right] k_{\text{B}} T \quad (23)$$

Here the first term gives the total number of fixed DNA charges that are within the micelle counterion atmosphere. These charges replace the counterions condensed on the micelle leading to an $\Omega k_{\text{B}}T$ contribution for each released ion. Also counterions of the DNA in the contact region are released. The factor $1 - b/l_{\text{B}}$ accounts for the fact that only a fraction of the fixed charges is neutralized by counterions (about 76%).

The wrapping of DNA around the micelle costs bending energy. According to the wormlike chain model¹ for one full turn wrap this amounts to

$$F_{\text{bend}}(m, n_C) = k_{\text{B}} T \frac{\pi l_p}{r(m, n_C) + r_{\text{DNA}}} \quad (24)$$

The overall complexation energy for the DNA–micelle aggregate is given by

$$F_{\text{compl}}(m, n_C) = F_{\text{release}}(m, n_C) + F_{\text{bend}}(m, n_C) \quad (25)$$

under the condition that $F_{\text{compl}} < 0$. If $F_{\text{compl}} > 0$ no complex forms; in such a case we set $F_{\text{compl}} = 0$ and the micelle size is assumed not to be affected by the presence of the DNA molecules. We checked that other terms like e.g. the interaction between the effective complex charge and the charges of the free DNA tail are much smaller and thus can be neglected. Note that the wrapped DNA typically overcharges the micelle (similar to the situation in a nucleosome¹). For instance, one DNA turn on a $n_C = 12$ -micelle with $n_{\text{max}} = 47$ is about 65 base pairs long carrying a total of 130 charges. We expect that the resulting net charge stabilizes the complexes against aggregation.

The distribution of micelle sizes is now given by

$$[Z_m] = [Z_1]^m e^{-[m\Delta F(m, n_C) + F_{\text{compl}}(m, n_C)]/k_{\text{B}}T} \quad (26)$$

This distribution is very different from that of the DNA-free case. As can be seen in Fig. 4 and 5 the size distribution is now bimodal since there are no micelles of intermediate size. This reflects the fact that when the first micelle–DNA complexes form, the bare micelles have on average still a very small size. On the

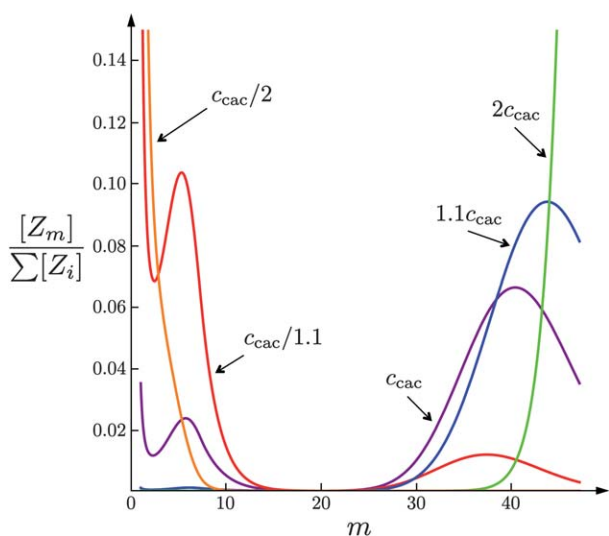


Fig. 4 Size distribution of micelles between $m = 1$ and $m_{\max} = 47$ for tail length $n_C = 12$ in the presence of DNA.

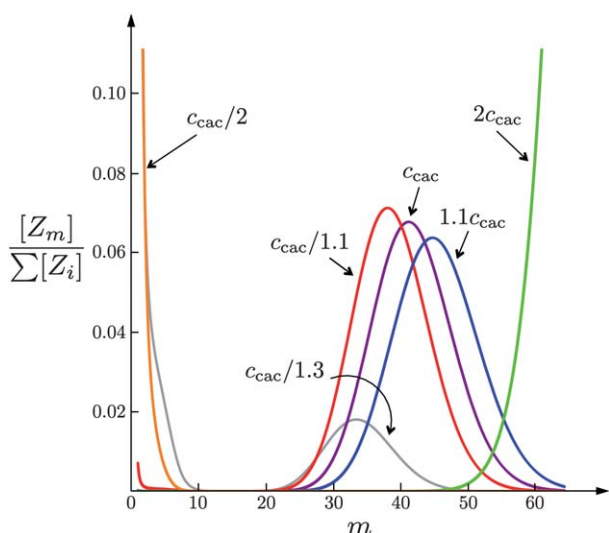


Fig. 5 Size distribution of micelles between $m = 1$ and $m_{\max} = 64$ for tail length $n_C = 14$ in the presence of DNA.

other hand, the complexes are much larger allowing for a smaller curvature of the wrapped DNA section.

We define the critical aggregation concentration (cac) similar to the definition of the cmc above, namely we require that at the cac the concentration of monomeric amphiphiles, $m = 1$, equals the concentration of the maximal micelles, $m = m_{\max}(n_C)$. In all the cases we studied we found that for such maximal micelles $F_{\text{compl}} < 0$, *i.e.*, they form indeed complexes. This leads to the following expression for the cac (up to terms of order m_{\max}^{-1}):

$$c_{\text{cac}} \equiv [Z_1] = \exp\left(\frac{\Delta F(m_{\max}, n_C) + F_{\text{compl}}(m_{\max}, n_C)}{k_B T}\right). \quad (27)$$

To a good approximation this fulfills again the Klevens equation, eqn (16) with B being given by eqn (17). There is, however, a small deviation from the linearity due to the

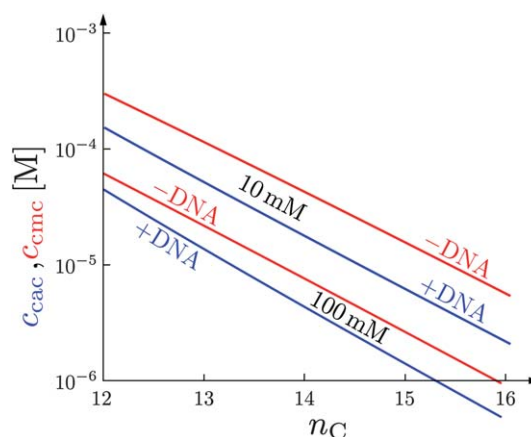


Fig. 6 Comparison between the cac and cmc for two different salt concentrations.

DNA-complexation contribution, $F_{\text{compl}}(m_{\max}, n_C)$ that has a complex dependence on n_C .

In Fig. 6 we compare the cac to the cmc, the latter is already presented in Fig. 3. The presence of DNA lowers substantially the concentration, *i.e.*, $c_{\text{cac}} \ll c_{\text{cmc}}$. In both the cases increasing the salt concentration has the same effect, namely lowering the concentration where the micelles form. However, this effect is reduced for the case when DNA is present. This reflects the fact that the release of counterions that drives the complex formation is less favorable for higher salt concentration as the entropic gain is reduced. However, the majority of counterions still needs to condense when micelle–DNA complexes form since the DNA can only make limited contact to the amphiphiles.

Note, however, the opposite dependence of cac on the salt concentration has been found experimentally,^{12,15} as mentioned in the Introduction. This might indicate that in these experiments the fraction of released counterions is larger than estimated here. This is to be expected if the contact area between DNA and the lipids is larger than in our model. This is, for instance, the case for DNA–cationic lipid complexes with inverted hexagonal geometry. Another example is a lamellar stack of lipid bilayers and parallel DNA double helices in between with membrane undulations that compress the stack,³⁸ a geometry that has been observed experimentally (J. O. Rädler, personal communication).

6 Conclusions

In this work we propose the formation of DNA-wrapped spherical cationic micelles as a possible alternative scenario for complex formation between DNA and cationic surfactants. The driving force for the complexation is the hydrophobic interaction between the surfactant tails and the release of condensed counterions from the micelle and the DNA. The rigidity of dsDNA counteracts DNA wrapping but can be energetically favorable on larger micelles. As a result the distribution of micelle sizes becomes bimodal in the presence of DNA. Aggregation happens at a concentration much smaller than the cmc, in agreement with experiments. Our theory, however, predicts that addition of salt lowers both the cmc and the cac whereas experiments find that only the cmc is lowered whereas the cac increases. The difference

in the experimentally observed dependencies of these concentrations on the ionic strength reflects the different roles that the counterions play during micelle formation (in the absence of DNA) and during complex formation: counterions have to condense on micelles but are released when complexes form. Even though our model accounts for all these effects, it predicts that the cac decreases with increasing salt. This is related to the fact that the contact area between a spherical micelle and wrapped DNA is so small that only a fraction of the counterions can be released. In the experimental systems one typically has very long DNA molecules that favor the formation of rodlike micelles that allow for a better contact between DNA and surfactants allowing for more complete counterion release.

It will be interesting to perform new experiments to investigate whether the proposed complexes between DNA and cationic surfactants can be formed. A possibility is to choose DNA of a length that is comparable to the wrapping length of a single spherical micelle. Another possible direction to pursue would be to use headgroups with a higher valency. This increases the interaction between DNA and surfactants. This lowers the cac and might favor the formation of the proposed complexes.

Acknowledgements

HS would like to thank the Japanese Society for the Promotion of Science for a JSPS Fellowship for Research in Japan that led to the current publication.

References

- H. Schiessel, *J. Phys.: Condens. Matter*, 2003, **15**, R699–R774.
- A. A. Zinchenko, K. Yoshikawa and D. Baigl, *Phys. Rev. Lett.*, 2005, **95**, 228101.
- A. A. Zinchenko, F. Luckel and K. Yoshikawa, *Biophys. J.*, 2007, **92**, 1318–1325.
- K. Hayakawa, J. P. Santerre and J. C. T. Kwak, *Biophys. Chem.*, 1983, **17**, 175–181.
- S. M. Mel'nikov, V. G. Sergeyev and K. Yoshikawa, *J. Am. Chem. Soc.*, 1995, **117**, 2401–2408.
- S. M. Mel'nikov, V. G. Sergeyev and K. Yoshikawa, *J. Am. Chem. Soc.*, 1995, **117**, 9951–9956.
- S. M. Mel'nikov, V. G. Sergeyev, K. Yoshikawa, H. Takahashi and I. Hatta, *J. Chem. Phys.*, 1997, **107**, 6917–6924.
- J. O. Rädler, I. Koltover, T. Salditt and C. R. Safinya, *Science*, 1997, **275**, 810–814.
- I. Koltover, T. Salditt, J. O. Rädler and C. R. Safinya, *Science*, 1998, **281**, 78–81.
- V. G. Sergeyev, S. V. Mikhailenko, O. A. Pyshkina, I. V. Yaminsky and K. Yoshikawa, *J. Am. Chem. Soc.*, 1999, **121**, 1780–1785.
- R. Dias, S. Melnikov, B. Lindman and M. G. Miguel, *Langmuir*, 2000, **16**, 9577–9583.
- V. A. Izumrudov, M. V. Zhiryakova and A. A. Goulko, *Langmuir*, 2002, **18**, 10348–10356.
- D. Matulis, I. Rouzina and V. A. Bloomfield, *J. Am. Chem. Soc.*, 2002, **124**, 7331–7342.
- R. S. Dias, A. A. C. C. Paisa, M. G. Miguela and B. Lindman, *Colloids Surf., A*, 2004, **250**, 115–131.
- D.-M. Zhu and R. K. Evans, *Langmuir*, 2006, **22**, 3735–3743.
- S. Rudiuk, S. Franceschi-Messant, N. Chouini-Lalanne, E. Perez and I. Rico-Lattes, *Langmuir*, 2008, **24**, 8452–8457.
- A. Diguët, N. K. Mani, M. Geoffroy, M. Sollogoub and D. Baigl, *Chem.–Eur. J.*, 2010, **16**, 11890–11896.
- S. Rudiuk, K. Yoshikawa and D. Baigl, *J. Colloid Interface Sci.*, 2012, **368**, 372–377.
- T. Wallin and P. Linse, *Langmuir*, 1996, **12**, 305–314.
- T. Wallin and P. Linse, *J. Phys. Chem.*, 1996, **100**, 17873–17880.
- T. Wallin and P. Linse, *J. Phys. Chem. B*, 1997, **101**, 5506–5513.
- A. Laguerre, S. Stoll, G. Kirton and P. L. Dubin, *J. Phys. Chem. B*, 2003, **107**, 8056–8065.
- T. Wallin and P. Linse, *Langmuir*, 1998, **14**, 2940–2949.
- S. Zhou, G. Liang, C. Burger, F. Yeh and B. Chu, *Biomacromolecules*, 2004, **5**, 1256–1261.
- S. May and A. Ben-Shaul, *J. Phys. Chem. B*, 2001, **105**, 630–640.
- A. Bernheim-Groswasser, R. Zana and Y. Talmon, *J. Phys. Chem. B*, 2000, **104**, 4005–4009.
- V. M. Jadhav, R. Valaske and S. Maiti, *J. Phys. Chem. B*, 2008, **112**, 8824–8831.
- D. Santhiya and S. Maiti, *J. Phys. Chem. B*, 2010, **114**, 7602–7608.
- C. Tanford, *J. Phys. Chem.*, 1974, **78**, 2469–2479.
- I. Rouzina and V. A. Bloomfield, *J. Phys. Chem.*, 1996, **100**, 9977–9989.
- H. Schiessel, R. F. Bruinsma and W. M. Gelbart, *J. Chem. Phys.*, 2001, **115**, 7245–7252.
- G. Gunnarsson, B. Jönsson and H. Wennerström, *J. Phys. Chem.*, 1980, **84**, 3114–3121.
- D. F. Evans, D. J. Mitchell and B. W. Ninham, *J. Phys. Chem.*, 1984, **88**, 6344–6348.
- R. Nagarajan and E. Ruckenstein, *Langmuir*, 1991, **7**, 2934–2969.
- V. Srinivasan and D. Blankshtein, *Langmuir*, 2003, **19**, 9932–9945.
- H. Kleven, *J. Am. Oil Chem. Soc.*, 1953, **30**, 74–80.
- A. J. Konop and R. H. Colby, *Langmuir*, 1999, **15**, 58–65.
- H. Schiessel and H. Aranda-Espinoza, *Eur. Phys. J. E: Soft Matter Biol. Phys.*, 2001, **5**, 499–506.